Status of GRS 1915 observations, November 1999

Reba Bandyopadhyay, Berrie Giebels

This note gives the state of the microquasar GRS 1915 observations by USA, up to DOY 214. No data have been taken in Epoch 1 after this date. However, USA has begun observing GRS1915+105 again as of Day 312 (8 November).

0.1 Data available

A look at the obspluswide yields table 0.1. Epoch 1 data are divided into 4 different intervals which correspond to the different pointer offsets in that Epoch.

DOY	Interval	Mode	Filename
179	2	M:1	SR01770_3_Y1999_D179_0941.usa.hkp
179	2	M:1	SR01772_4_Y1999_D179_1307.usa.hkp
179	2	M:1	SR01774_4_Y1999_D179_1632.usa.hkp
180	2	M:1	SR01785_3_Y1999_D180_1104.usa.hkp
180	2	M:1	SR01787_2_Y1999_D180_1410.usa.hkp
180	2	M:1	SR01789_1_Y1999_D180_1723.usa.hkp
181	2	M:1	SR01799_3_Y1999_D181_1047.usa.hkp
181	2	M:1	SR01800_4_Y1999_D181_1233.usa.hkp
181	2	M:1	SR01802_4_Y1999_D181_1559.usa.hkp
192	2	M:2	SR01950_3_Y1999_D192_0228.usa.hkp
201	2	M:2	SR02091_0_Y1999_D202_0047.usa.hkp
202	2	M:2	SR02093_0_Y1999_D202_0434.usa.hkp
202	2	M:2	
202	2	M:1	
202	2	M:1	
213	3	M:2	SR02252_3_Y1999_D213_1004.usa.hkp
214	3	M:2	SR02265_2_Y1999_D214_0753.usa.hkp
214	3	M:2	SR02266_3_Y1999_D214_0945.usa.hkp
214	3	M:2	SR02266_3_Y1999_D214_0945.usa.hkp
214	3	M:2	SR02268_0_Y1999_D214_1313.usa.hkp

Table 1: Observations of GRS 1915 in Epoch 1.

0.2 Brief description of data

A broad sample of lightcurves for different observations of GRS1915 are in Figures 1 to 7.

In general, the data between DOY 179-181 show GRS1915+105 to be in a steady, non-flaring state. Please note that during this interval we were not only using the wrong yaw offset but also there was a small error in the coordinates of GRS1915+105 as entered into the target database. Therefore the count rates we observed were significantly lower than the actual flux from the source, as can be determined by examining the RXTE ASM light curves from the same interval. These fluxes have been corrected using the rate correction factors[1].

During days 201 and 202 GRS1915+105 appears variable on a timescale of several hundred seconds, varying between ~750-1500 counts. An abrupt change in the behaviour of GRS1915+105 then occurs between UT 4:59:22 and 6:34:48 on day 202. The source begins to exhibit very distinctive but non-periodic flares, with the interval between flares appearing to vary between ~100-160 seconds, and having slow raise and sharp decay. Our next observations, on days 213-214, show that GRS1915+105 has remained in this flaring state; however, the interval between flares has shortened to ~60-80 seconds. According to the ASM, this state persists until around day 218, when the source becomes relatively steady once again. The USA data therefore clearly constrain the beginning of these oscillations to the 90 minute interval between our last two observations of GRS1915+105 on day 202.

[1] These rate correction factors pertain to the source, but they increase the noise level. This is not very important in the high intensity regime

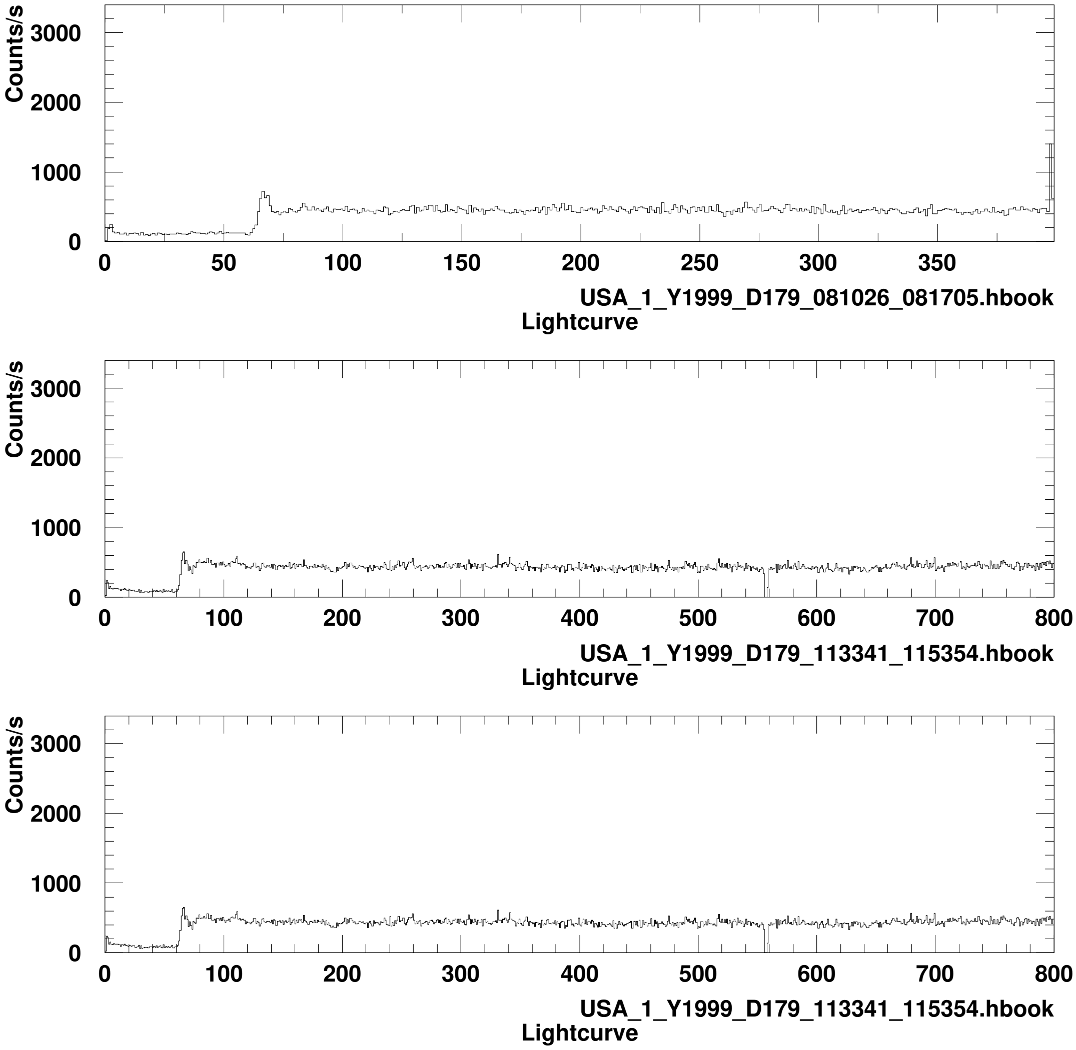

Figure 1: Lightcurves for the GRS observations in Epoch 1. No remarkable features are present in the lightcurve up to DOY202.

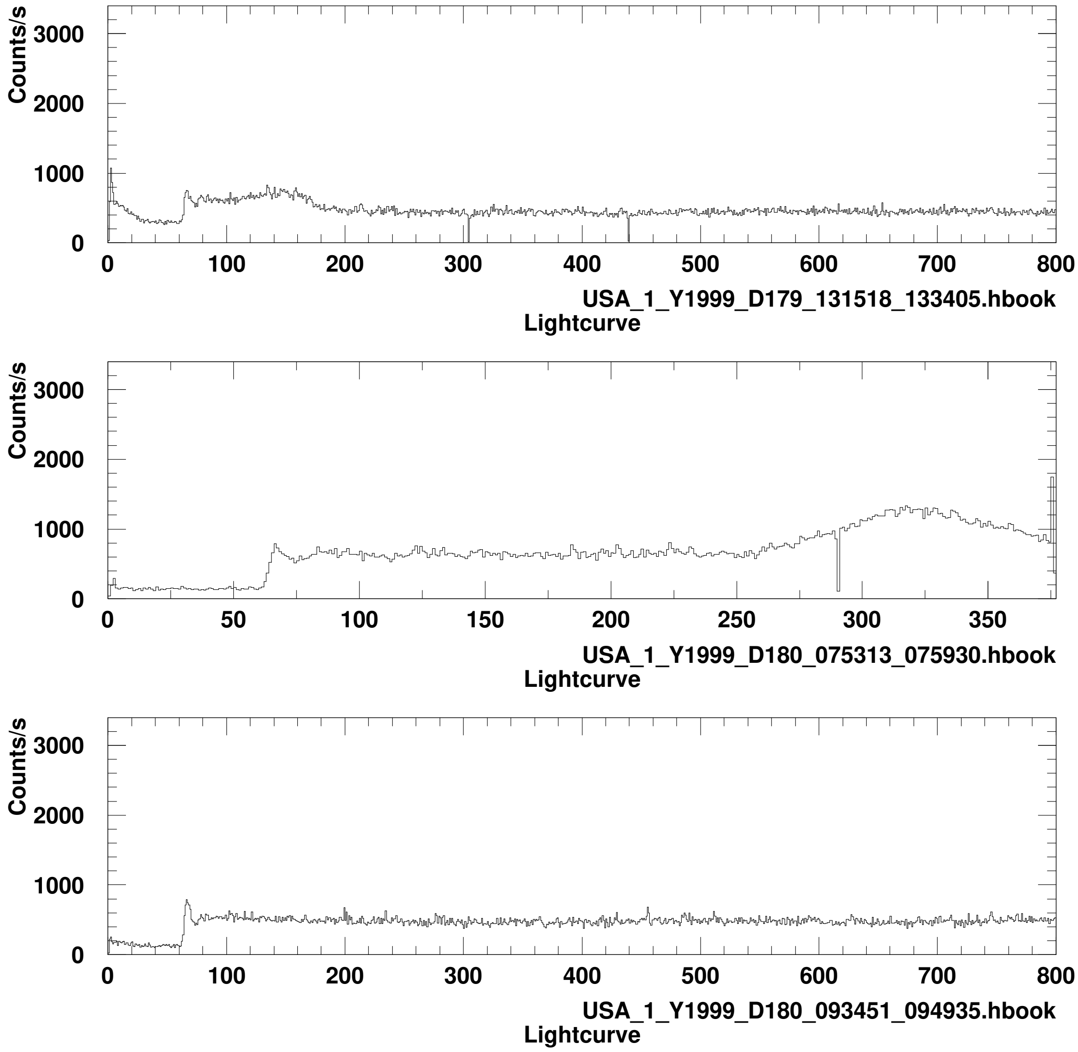

Figure 2: Lightcurves for the GRS observations in Epoch 1.

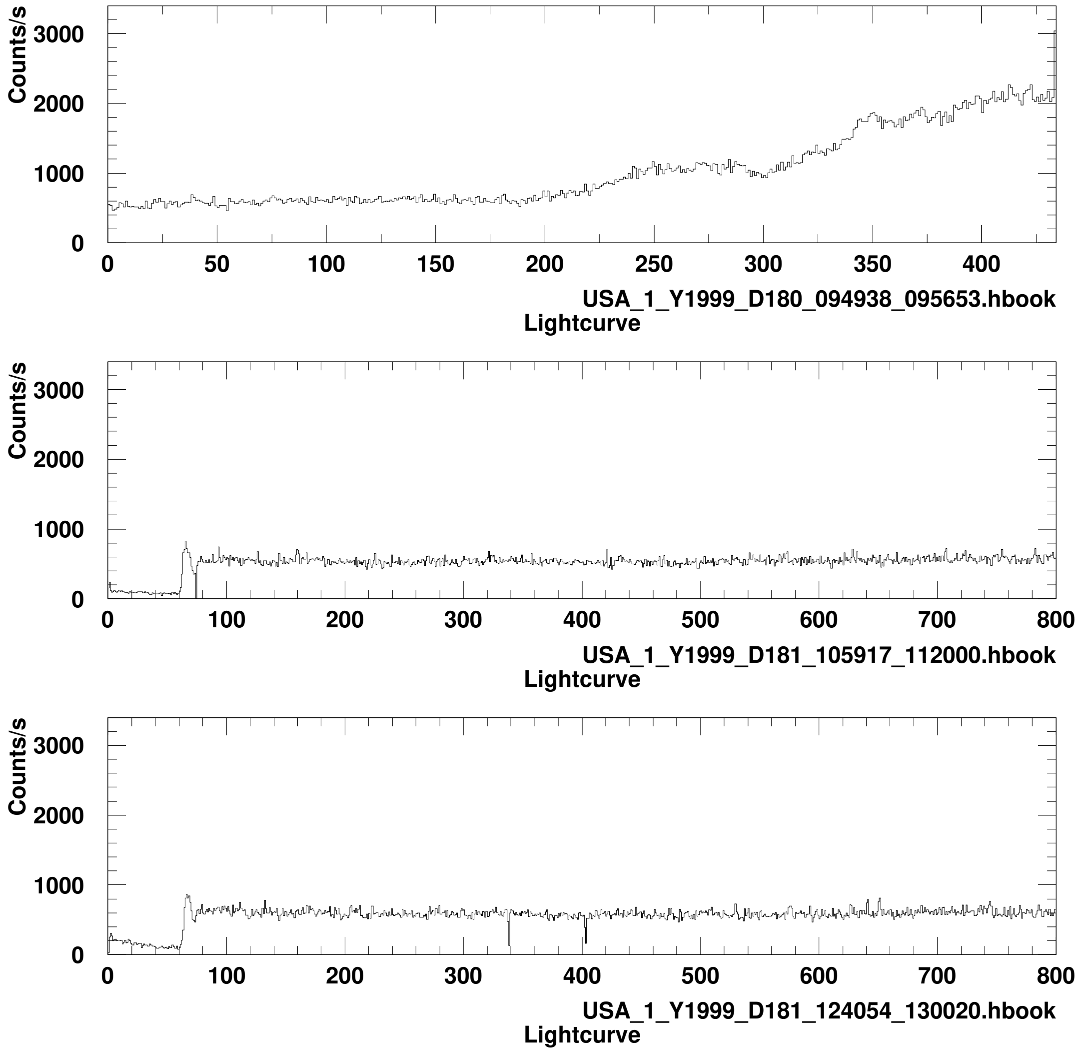

Figure 3: Lightcurves for the GRS observations in Epoch 1.

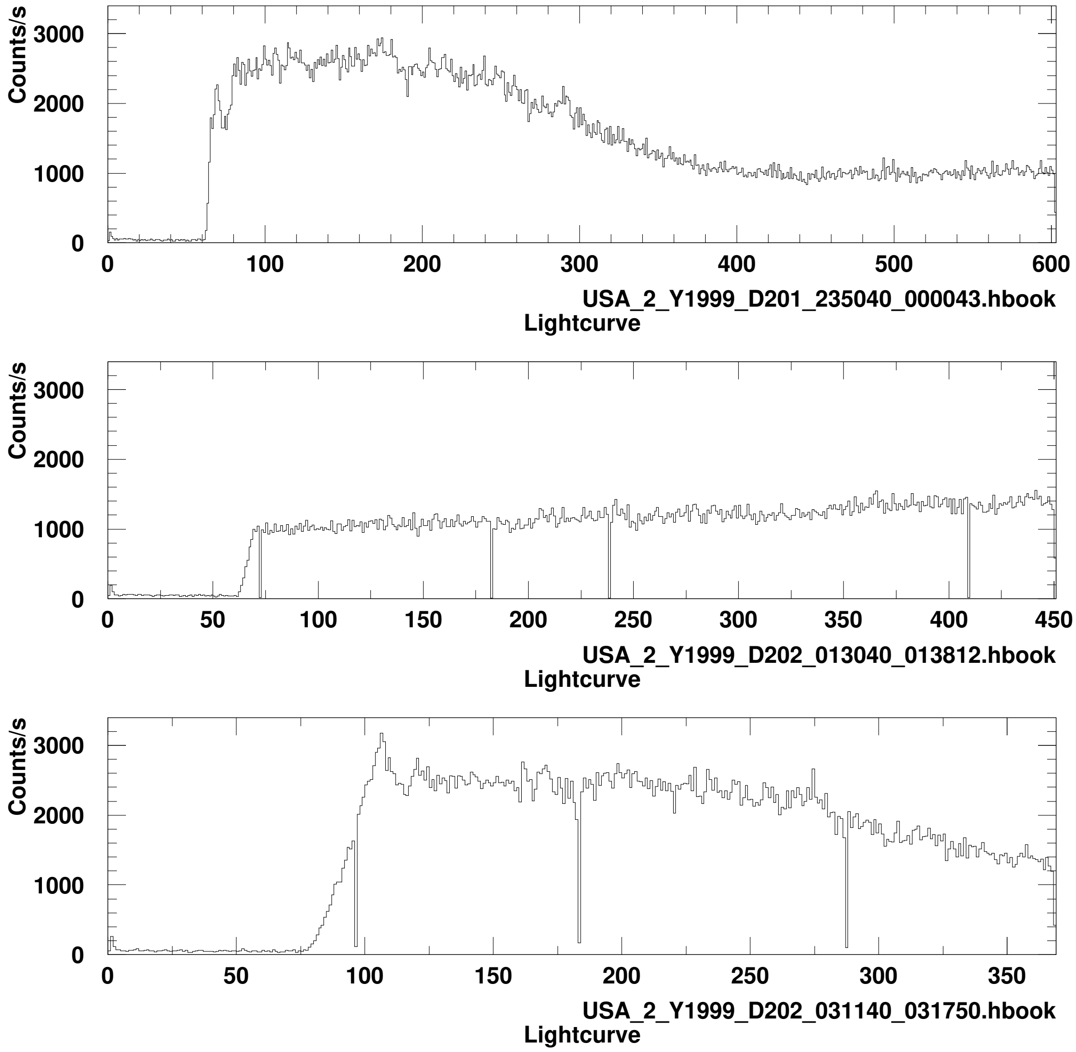

Figure 4: Lightcurves for the GRS observations in Epoch 1.

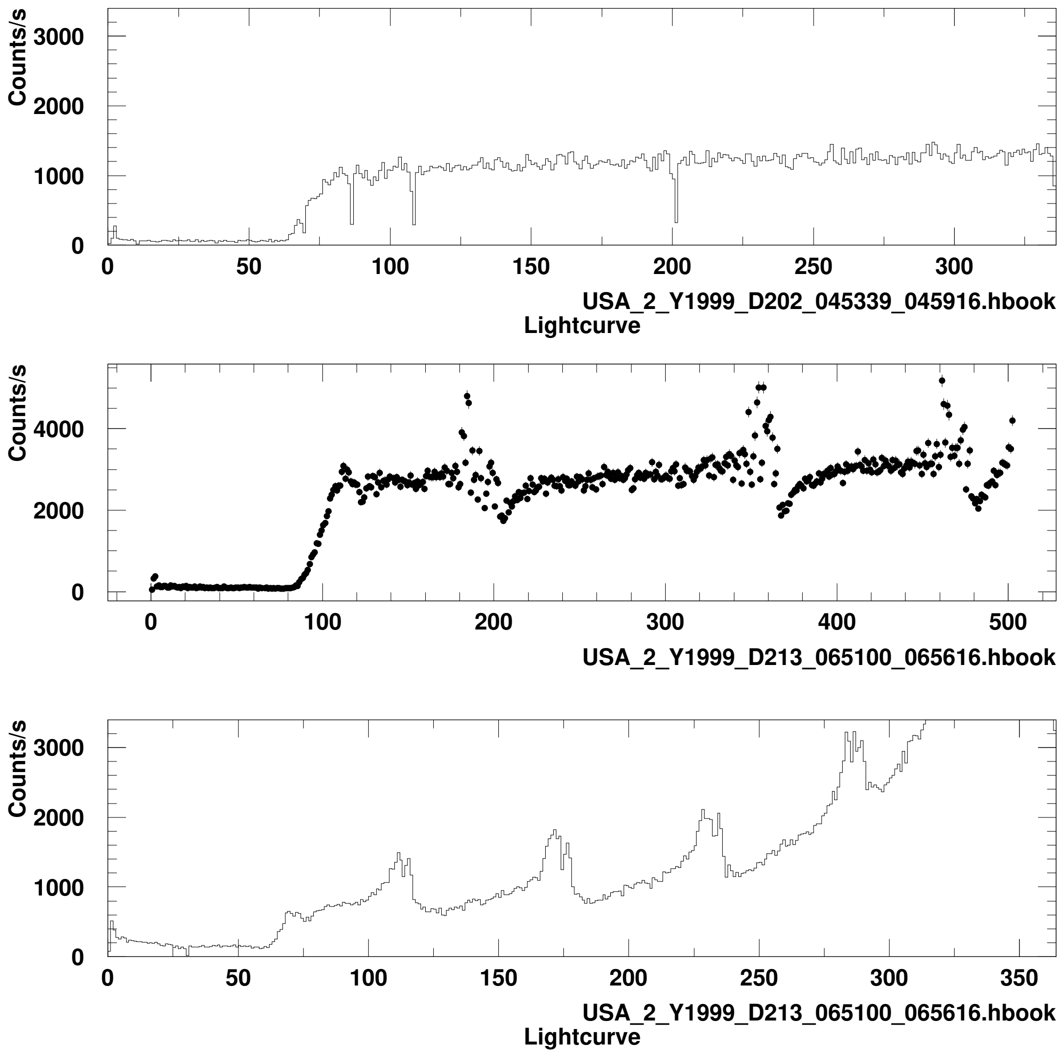

Figure 5: Lightcurves for the GRS observations in Epoch 1. The oscillation appears in the middle plot but not approximately 2 hours before. The filename of the middle plot is wrong and should be D202_063452_064315.

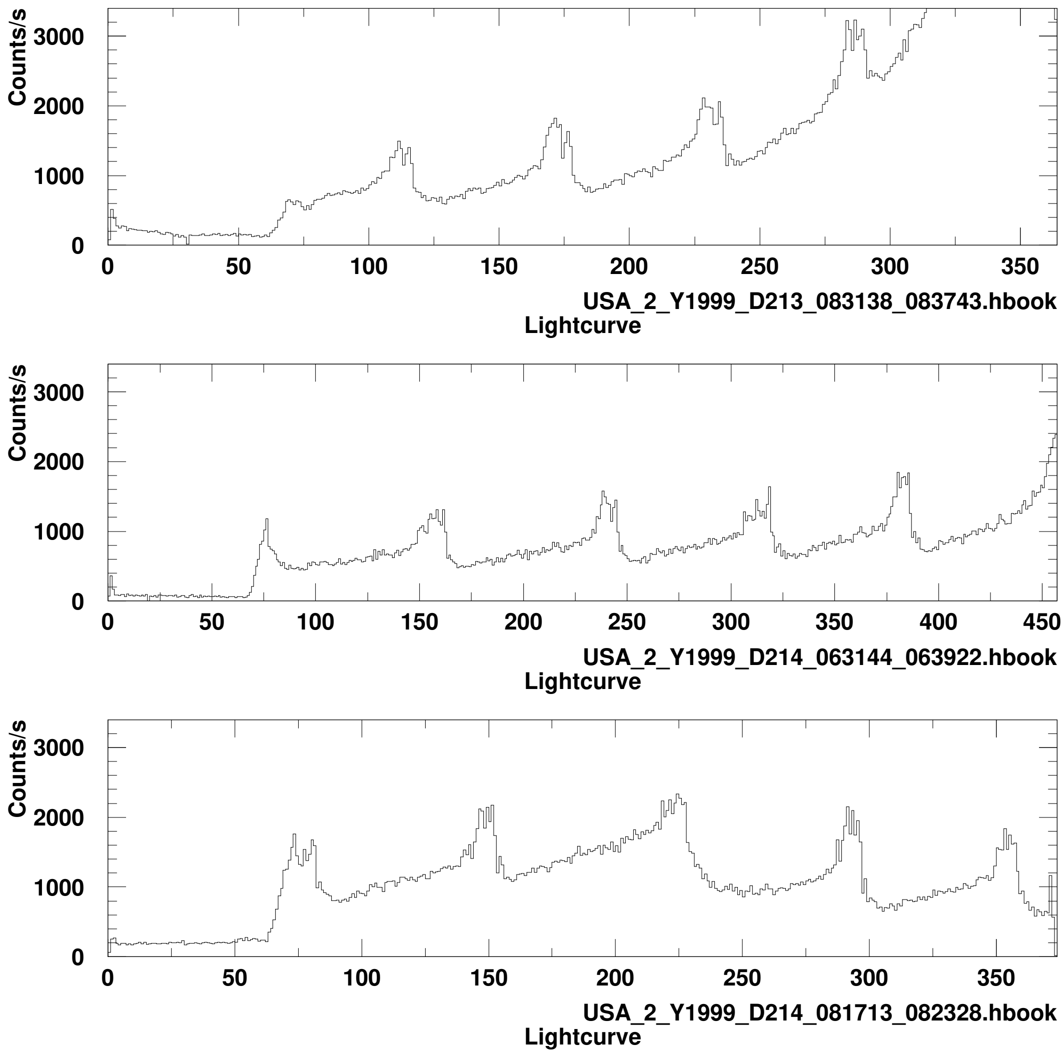

Figure 6: Lightcurves for the GRS observations in Epoch 1. The rate increase visible in the top and bottom plots are correlated with an increase in all the veto rates, and thus are very likely to be due to noise.

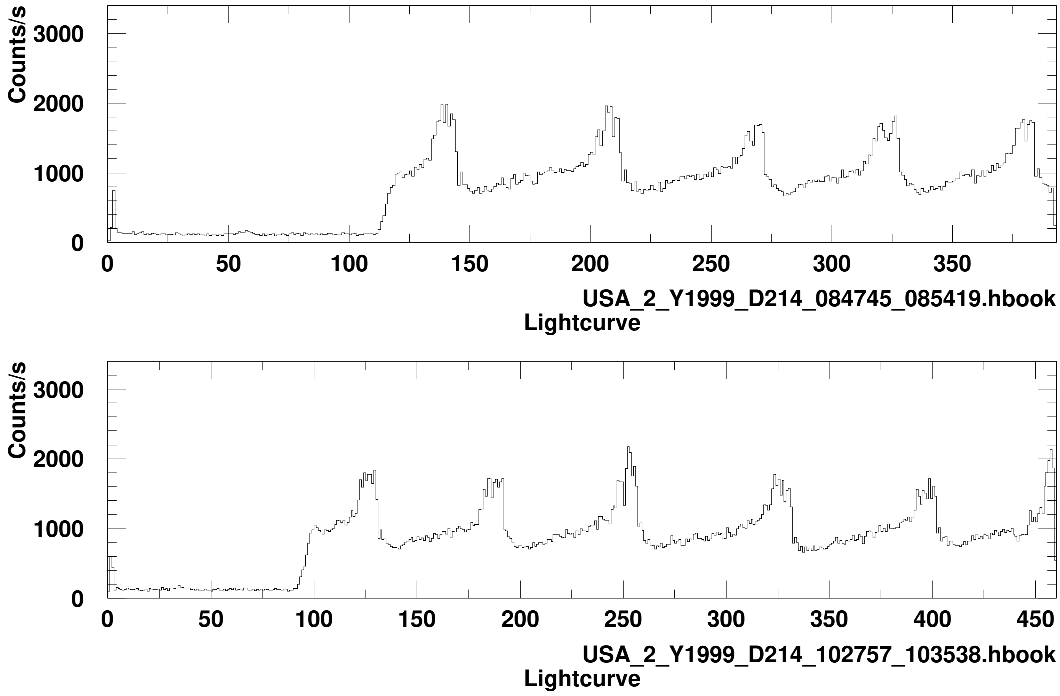

Figure 7: Lightcurves for the GRS observations in Epoch 1.

0.3 Search for mHz-Hz QPO's

0.3.1 In Mode 1 Data

Most of the data present a counting rate that can exceed 1000 Hz, thus the gaps appear in the Power Density Spectra (PDS). Recently Kaice made a FFT tool available that copes with the gap problem in mode 1. The FFT's are taken in 0.7 seconds segments, which means that the lowest resolution achievable is a Nyquist frequency of $f_c = 1.42$ Hz. So far none of the mode 1 data have been analyzed.

0.3.2 In Mode 2 Data

The latest data in Epoch 1 were taken in mode 2, where the gaps are not present. During these observations, a QPO at sub-Hz frequency is visible in the lightcurve. All the bursts here start with a well defined sharp peak and decay faster than they rise. Assuming that the oscillating state does not change over the DOY213-214 period just one PDS study was made on the latest observation available on DOY214 (See bottom lightcurve in Fig 7). A PDS is estimated for the whole lightcurve (Fig 8) and also dynamic PDS (with 4 second time intervals) in Fig 9. For comparison a dynamic PDS is shown for the Crab nebula (Fig 10).

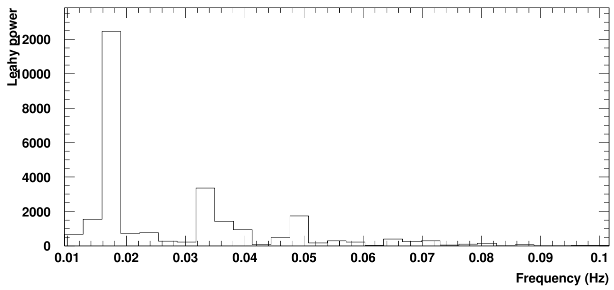

Figure 8: Leahy normalized PDS for the data shown in the bottom lightcurve of Fig.7, for data between t = 100 s and t = 450 s. The peak at 0.016 Hz corresponds to the 60 second QPO which is visible in the lightcurve.

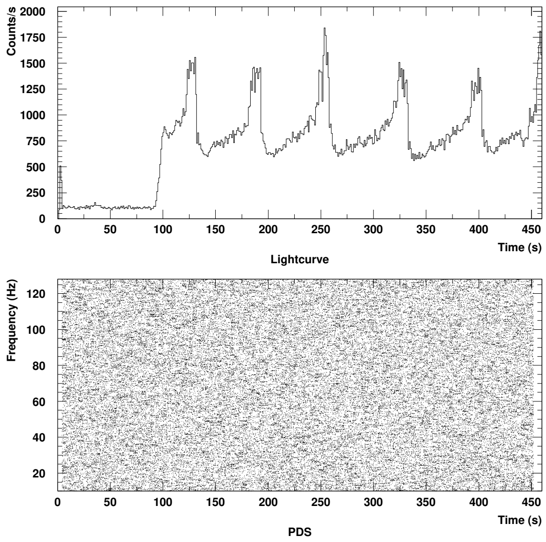

Figure 9: Dynamic PDS of the lightcurve shown at top. No obvious QPO is visible at frequencies above 1 Hz.

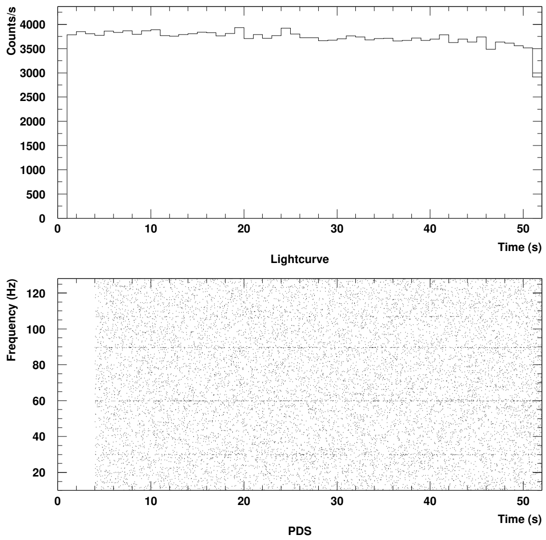

Figure 10: Dynamic PDS for the Crab pulsar. The stable 30 Hz and harmonics are visible.

0.4 Spectroscopy and Hardness ratio

0.4.1 In Mode 2 data

The data from which are extracted the 2 bottom lightcurves of Fig(7) have a stable background (coincidence veto, particle veto rates are stable over the major part of the observation). These observations are at the present moment the most secure for spectral analysis purposes, since the background collected before USA points towards the source can be used to make in XSPEC a background PHA file for the whole observation.

The hardness ratio is shown in Fig(11) as a function of time in 2 seconds bins. The ratio is defined here as the ratio in the raw PHA channels 9-14 to the rate in 1-8, using the numbering convention 0-15. This must be approximately 1keV-10keV / 10keV-22keV. The lowest and the highest channels were not used, since the lowest channel is supposed to cover energies below 1 keV, where the acceptance is not well known, and the highest channels contains the energy overflows.

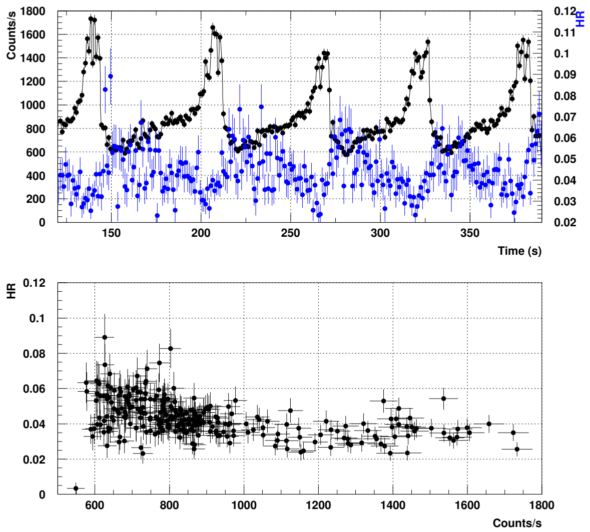

Figure 11: Upper plot: Hardness ratio as defined in the text and source intensity as a function of time for the last observation of DOY214. The hardest state is reached at the very end of a flare. Bottom plot: Hardness ratio as a function of intensity. Two distinct populations seem to appear but this needs more statistical evidence.

According to Yadav *et al* (ApJ June 1999 astro-ph/9901055, Yadav hereafter), above 10keV the power-law component is supposed to dominate. In the 1-10 keV range the Shakura-Sunyaev multi-temperature disk emission is supposed to dominate. The hardest state is reached at the *end* of the peak in intensity. In the same figure the hardness as a function of intensity is shown.

The different components of the lightcurve described in section 0.3.2 are fitted by an absorbed powerlaw model. Power law index versus sequence[2] number are shown in Fig(12). The emitted radiation tends to become harder after the peak emission has occured. The absolute numbers could change in the future since an older version of the response matrix was used here. The spectral index of the fitted power-law after the maximum of the burst varies between 2.2 and 2.4, indicating that the source is in a hard state. During the burst state the intensity is higher and the power-law index is steeper (between 2.7 and 2.9). In a scenario sketched by Yadav the X-ray bursts are due to fast changes in the spectral states when the source reaches the high state and the accretion rate is very close to the Eddington accretion rate. Jet formation may be setting in during the bursting period.

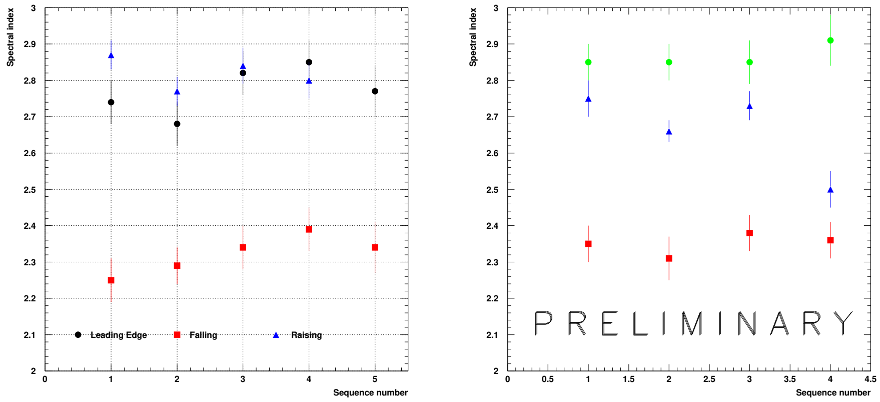

Figure 12: Power law index for the different components in the lightcurve of Fig(7). Left plot: the middle lightcurve of Fig(7), Right plot: the bottom lightcurve of Fig(7).

0.4.2 In Mode 1 data

The first strong oscillation is observed in mode 1 at DOY202, as can be seen in Fig(5). The same plots as for the previous subsection have been made here

[2]A sequence is defined here as being a fast *leading edge* in the peak, followed by a fast *falling edge* and a slower *raising edge*.

(Fig(13)). The hardness ratio is at the same scale as previously and appears to be higher. For comparison the same plots are shown for a steady state in DOY180 (Fig(14)).

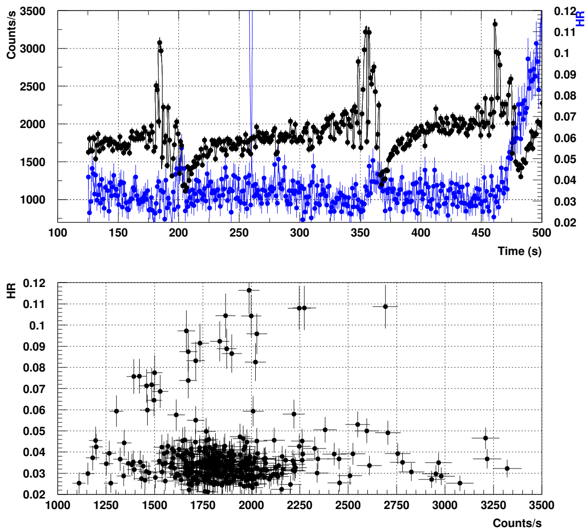

Figure 13: Upper plot: Hardness ratio as defined in the text and source intensity as a function of time for the DOY202 where strong oscillations appear. The hardest state is reached at the end of a flare. The increase in HR at the end of the observation is correlated with veto rates.

0.5 Comparison with XTE observations and discussion

A similar oscillation as in DOY 214 has been seen by XTE in 1998 and is discussed in Yadav. The oscillations are due to change in the disk accretion rate which may be either due to a change in the total accretion rate or due to some changes in the viscosity in the thin accretion disk.

0.6 Simultaneous multi-wavelength data

Much of the Epoch 1 USA data of GRS1915+105 was taken in conjunction with a variety of IR and other multi-wavelength observing campaigns. The data from

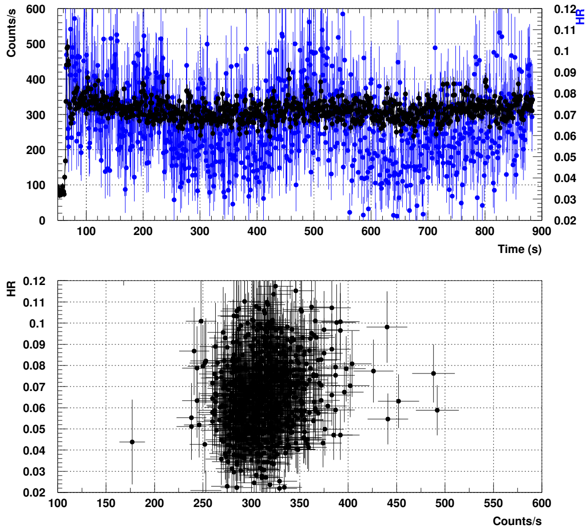

Figure 14: Upper plot: Hardness ratio as defined in the text and source intensity as a function of time for the DOY180 where no oscillations are visible.

days 179-181 were taken simultaneously with IR fast photometry at Palomar and XTE observations obtained by Steve Eikenberry (Cornell). The day 202 data was taken as part of a large collaborative campaign which included VLT IR spectroscopy, radio monitoring, and XTE observations. Finally, the day 213-214 observations were coordinated with simultaneous IR spectroscopy obtained at UKIRT by Tariq Shahbaz (Oxford). The multi-wavelength data from all three campaigns are currently under reduction by the respective groups, and the USA data will be eventually be combined with those data for analysis of the multi-wavelength behaviour of GRS1915+105.

A brief summary of what multi-wavelength campaigns on GRS1915 have provided:

- **X-ray and IR photometry** observations have provided what might be the first evidence for a time-dependent disk-jet interaction (Eikenberry ApJ Feb 1998).
- **X-ray and IR spectroscopy** showed that emission-line fluxes varied in approximately linear proportionality to the IR continuum flux, and provided further evidence that the IR flares signify the ejection of material out of the accretion disk plane (Eikenberry ApJ October 1998).
- Simultaneous **X-ray and radio** lightcurves showed evidence for a tem-

porary disappearance and subsequent restoring of the inner portion of the accretion disk during the flare (Feroci 1999 astro-ph/9909465).

Also recent radio flares of GRS1915 have been observed by NRAO. Figure 15 shows the radio flares occuring November 15th and 17th. The boxes indicate scheduled USA observations that have not yet been downloaded.

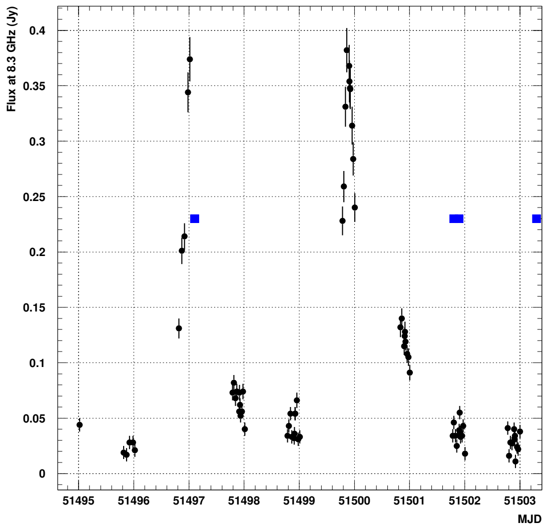

Figure 15: Radio fluxes at 8.3 GHz of GRS1915 as measured by NRAO. The peaks correspond to Nov.15th and 17th. The boxes indicate scheduled USA observations.